Eur Radiol (2014) 24:209–213
DOI 10.1007/s00330-013-2999-3

UROGENITAL

Increased signal intensity of prostate lesions on high *b*-value diffusion-weighted images as a predictive sign of malignancy

Michael Quentin · Lars Schimmöller · Christian Arsov · Robert Rabenalt · Gerald Antoch · Peter Albers · Dirk Blondin

Received: 22 May 2013 / Revised: 10 July 2013 / Accepted: 7 August 2013 / Published online: 31 August 2013

Abstract
Objectives The evaluation of lesions detected in prostate magnetic resonance imaging (MRI) with increased signal intensity (SI) on high *b*-value diffusion-weighted images as a sign of malignancy.
Methods One hundred and three consecutive patients with prostate MRI examination and MRI-guided in-bore biopsy were retrospectively included in the study. MRI-guided in-bore biopsy histologically confirmed prostate cancer in 50 patients ($n=92$ lesions). The other 53 patients ($n=122$ lesions) had negative bioptical results.
Results In patients with histologically confirmed prostate cancer, 46 of the 92 lesions had visually increased SI on the high *b*-value images compared with the peripheral zone (SI=+27±16%) or the central gland (SI=+37±19%, $P<0.001$ respectively). In patients with a negative biopsy, ten of the 122 lesions had visually increased SI (compared with the peripheral zone, SI=+29±18%, and with the central gland, SI=+41±15%, $P<0.001$ respectively). Neither the apparent diffusion coefficient (ADC) values nor the Gleason Score of lesions with increased SI were significantly different from lesions without increased SI.
Conclusions Visually increased SI on the high *b*-value images of diffusion-weighted imaging using standard *b*-values is a sign of malignancy but can occasionally also be a feature of benign lesions. However, it does not indicate more aggressive tumours.
Key points
- *Diffusion weighted magnetic resonance imaging is increasingly used to diagnose prostatic cancer*
- *Reduced signal intensity (SI) on apparent diffusion coefficient (ADC) mapping is characteristic*
- *Prostatic tumours usually exhibit increased SI on high b-value images*
- *But benign lesions can also yield increased SI on high b-value images*

Keywords Prostate cancer · MRI · Diffusion-weighted imaging · High *b*-value · PI-RADS

Abbreviations

ADC	apparent diffusion coefficient
DCE-MRI	dynamic contrast-enhanced magnetic resonance imaging
DWI	diffusion-weighted imaging
MRSI	spectroscopy
PI-RADS	Prostate Imaging Reporting and Data System
SI	signal intensity

Introduction

Magnetic resonance imaging (MRI), combining anatomical imaging (T2-weighted images, T1-weighted images) with

M. Quentin · L. Schimmöller (✉) · G. Antoch · D. Blondin
Department of Diagnostic and Interventional Radiology, University Dusseldorf, Medical Faculty, Moorenstr. 5, 40225 Dusseldorf, Germany
e-mail: lars.schimmoeller@med.uni-duesseldorf.de

M. Quentin
e-mail: Michael.Quentin@med.uni-duesseldorf.de

G. Antoch
e-mail: Antoch@med.uni-duesseldorf.de

D. Blondin
e-mail: Blondin@med.uni-duesseldorf.de

C. Arsov · R. Rabenalt · P. Albers
Department of Urology, University Dusseldorf, Medical Faculty, Moorenstr. 5, 40225 Dusseldorf, Germany

C. Arsov
e-mail: christian.arsov@med.uni-duesseldorf.de

R. Rabenalt
e-mail: Robert.Rabenalt@med.uni-duesseldorf.de

P. Albers
e-mail: urologie@uni-duesseldorf.de

functional imaging, such as diffusion-weighted imaging (DWI), dynamic contrast-enhanced MRI (DCE-MRI) and spectroscopy (MRSI), is increasingly used for the diagnosis of prostate cancer. Functional imaging techniques are known to increase both the sensitivity and specificity of prostate MRI [1]. In 2012 the European Society of Urogenital Radiology (ESUR) published guidelines for the standardisation, evaluation and reporting of prostate MRI [2]. These guidelines include a scoring system named PI-RADS (Prostate Imaging Reporting and Data System) for the evaluation of prostate lesions. In DWI a reduced signal intensity (SI) on the apparent diffusion coefficient (ADC) map is indicative of prostate cancer [3]. The ESUR guidelines also mention the increased SI of a lesion on the high *b*-value images of DWI. For scoring DWI, a lesion with a reduced ADC value and non-increased SI on high *b*-value images is given 4 out of 5 possible points in the PI-RADS score, whereas a lesion with reduced ADC value but increased SI obtains 5 points. Therefore these lesions will receive a higher suspicious score. The reduced signal on the ADC map of suspect lesions may be considered standard knowledge and is routinely applied in the clinical practice. To the best of our knowledge, an increased SI on the high *b*-value images of diffusion-weighted prostate MRI of suspect lesions has not yet been systematically evaluated separately, and this is the aim of the present study.

Materials and methods

Patients

The study was approved by the local ethics committee. A total of 103 consecutive patients who underwent prostate MRI examination and MRI-guided in-bore biopsy between July and November 2012 were retrospectively included in the study. MRI-guided in-bore biopsy confirmed prostate cancer in 50 patients ($n=92$ lesions). In these patients only the confirmed malignant lesions were analysed. Lesions with negative histopathological finding were not analysed in these patients since prostate cancer is a multifocal tumour and an absolute "gold standard" is missing to define these lesions as true-negative findings. In 53 patients ($n=122$ lesions) the biopsy results were negative for tumour.

Diffusion-weighted imaging

The prostate MRI examinations were acquired on a 3-T MRI (Magnetom Trio; Siemens Medical Systems, Erlangen, Germany) with a six-channel phased-array body-coil. DWI was performed using a single-shot spin-echo echo-planar sequence (TR 4,600 ms, TE 90 ms, FOV 20.4 cm, voxel size 1.5×1.5×3.0 mm, image matrix 136×136, using a GRAPPA parallel imaging scheme with an acceleration factor of 2 and an acquisition time of 7:12 min). To acquire diffusion-weighted images, five *b* values (0, 250, 500, 750, 1,000 s/mm^2) with five averages, applying diffusion gradients in three orthogonal directions for each *b* value, were used. The ADC parameter maps were acquired by the MRI software using the standard monoexponential model.

MRI-guided in-bore biopsy

For each patient, a maximum of three different lesions were defined, selecting the most malignant lesions, as described previously [4]. These lesions involved malignant and benign findings. To select the lesions, a combination of T2-weighted imaging, DWI and DCE-MRI was used. In-bore MR-guided biopsies in all defined lesions were performed on the same 3-T MRI (Magnetom Trio; Siemens Medical Systems, Erlangen, Germany) transrectally with the patient in the prone position. The dynatrim biopsy device (Invivo, Orlando, FL, USA) and the corresponding software DynaCAD (Invivo, Orlando, FL, USA) was used for targeting. For biopsy planning a six-channel phased-array body-coil was placed on the back of the patient gaining fast T2-weighted HASTE images in the sagittal (TE 76 ms, FOV 28 cm, voxel size 1.4×1.1×3.0 mm) and axial (TE 76 ms, FOV 28 cm, voxel size 1.4×1.1×3.0 mm) planes. Two tissue samples of each lesion were obtained with an MR-compatible biopsy gun (Invivo, Orlando, FL, USA).

Measurements

ADC values and signal intensities on the high *b*-value (1,000 s/mm^2) images of the peripheral zone, the central gland and the defined lesions were evaluated using ROI-based measurements on workstations using the picture archiving and communication system (PACS). Round ROIs were defined as large as possible by a radiologist with 4 years' experience in prostate MRI. To evaluate the peripheral zone and the central gland, the measurements were repeated three times in different areas. ROIs were copied from the ADC map to the high *b*-value images to ensure that the same lesions were measured using the PACS. In addition to the measurements a radiologist experienced in reading prostate MRI assessed whether the lesions had visually increased SI on the high *b*-value images. As measured signal intensity values in MRI do not represent absolute data these values were used objectively as relative differences in the same patient. The different lesions were analysed regarding their localisation.

Statistics

All data are expressed as mean ± standard division. The statistical analysis was performed using IBM SPSS Statistics 19 for Windows (SPSS, Chicago, IL, USA). Statistical

significance was defined as a P value below 0.05. The data were tested for normal distribution using the Kolmogorov–Smirnov test. Normally distributed parameters were compared using the independent sample t-test. Correlation coefficients were calculated between ADC values and the SI on the high b-value images.

Results

One hundred and three patients (mean age 67 years, range 47–83 years) were retrospectively included. Fifty-three patients had histologically confirmed prostate cancer in 92 lesions. The tumour lesions were distributed as follows: 20 with Gleason Score 3+3=6, 52 with Gleason Score 3+4=7, 12 with Gleason Score 4+3=7, 4 with Gleason Score 4+4=8 and 4 with Gleason Score 4+5=9. Forty-eight of these tumours were located in the peripheral zone, 33 centrally and the other 11 in the anterior fibromuscular stroma. Fifty-three patients had negative biopsies in 122 lesions.

In the patients with confirmed prostate cancer, 46 out of 92 lesions had visually increased SI on the high b-value (1,000 s/mm^2) images (Fig. 1). These 46 lesions showed higher SI than the corresponding peripheral zone (+27±16%) or central gland (+37±19%, Table 1). Thirty out of 46 lesions with visually increased SI on the high b-value images were located in the peripheral zone.

In patients with a negative biopsy, ten out of 122 lesions had visually increased SI on the high b-value images (Fig. 2). Two of these lesions were located in the peripheral zone, one in the anterior fibromuscular stroma and the other seven centrally. The SI was 29±18% and 41±15% higher than the SI in the peripheral zone and the central gland, respectively. The increase in SI in the different lesions compared with the peripheral zone and the central gland was highly significant (P<0.001, respectively) compared with patients without visually increased SI on the high b-value images.

Overall, 56 lesions had increased SI on the high b-value images, including the 46 lesions with confirmed prostate cancer (82%). Tumour lesions with increased SI were not visually distinguishable from non-tumour lesions with increased SI on the high b-value images.

One of the patients with a lesion with increased SI in the central gland on the high b-value images and a negative biopsy received a laparoscopic adenectomy owing to severe bladder outlet obstruction. Histological assessment after adenectomy showed no prostate cancer in this patient, confirming the biopsy result.

In patients with and without prostate cancer, lesions with increased SI showed no significant difference in the ADC compared with lesions without increased SI on the high b-value images (P=0.57 for tumours, P=0.25 for benign lesions). There was only a weak correlation between ADC values and SI on the high b-value images (r=0.20 tumours, r=0.29 benign lesions). There was no significant difference (P=0.11) in the Gleason Score between lesions with and without increased SI on the high b-value images.

The ADC values of lesions with histologically confirmed prostate cancer (ADC=606±162×10^{-6} mm^2/s) were significantly lower (P<0.001) than those in patients with a negative biopsy (ADC=701±148×10^{-6} mm^2/s). The ADC values of the peripheral zone were significantly lower (P<0.005) in patients with prostate cancer (ADC=1,538±247×10^{-6} mm^2/s) compared with patients with a negative biopsy (ADC=1,664±196×10^{-6} mm^2/s), while the ADC values of the central gland did not differ significantly (P=0.48) (tumour group ADC=1,126±53×10^{-6} mm^2/s, non-tumour group ADC=1,151±50×10^{-6} mm^2/s).

Discussion

DWI is an integral part of functional prostate MRI [5]. The DWI depends on the microscopic mobility of water molecules, the "Brownian motion". This mobility is naturally restricted in

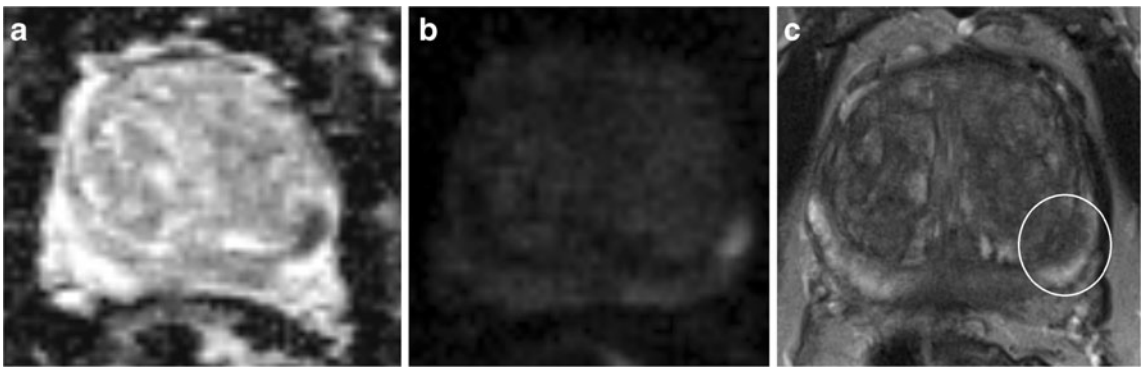

Fig. 1 A 68-year-old patient with a small peripheral prostate cancer (Gleason Score 9) proved by MRI-guided in-bore biopsy. **a** Apparent diffusion coefficient (ADC) map with reduced signal intensity (SI); **b** increased SI on the high b-value image (b=1,000 s/mm^2); **c** corresponding T2-weighted image of the tumour

Table 1 Signal intensity (*SI*) of hyperintense lesions compared with the peripheral zone or central gland in the same patient

	Patients (*n*)	Lesions (*n*)	Hyperintense lesions on high *b*-value images (*n*)	SI of hyperintense lesions compared with the peripheral zone	SI of hyperintense lesions compared with the central gland
Positive biopsy	53	92	46	+27±16%	+37±19%
Negative biopsy	50	122	10	+29±18%	+41±15%
Total	103	214	56	+28±16%	+38±18%

Number (*n*) of hyperintense lesions on high *b*-value images in the different groups (with positive or negative biopsy) and difference in SI compared with the peripheral zone or the central gland in each patient

tissue compared with pure water. From DWI the ADC can be calculated, reflecting the movement of the water molecules within the interpulse time [1]. The calculation algorithms are determined by the motion of the water molecules and are therefore influenced by the underlying structure of the tissue [6]. It is widely accepted that ADC values are predominantly reduced in prostate cancer compared with normal prostate tissue [3]. Prostate cancer replaces the normal glandular structure of the tissues and leads to a higher cell density, restricting the motion of water molecules [7, 8]. The recently released guidelines for prostate MRI from the ESUR also take into account the possible increased SI of prostate lesions on the high *b*-value diffusion-weighted images [2]. The *b* values express the amount of diffusion-weighting within the DWI pulse sequence. The scoring system of the ESUR guidelines, PI-RADS, assigns the maximum of five points to lesions that show both reduced SI in the ADC and increased SI on the high *b*-value images. These lesions therefore have a higher probability of being characterised as malignant.

We found that there are lesions with visually increased SI on the high *b*-value images showing significantly higher SI than the surrounding tissue (Fig. 1). These lesions were predominantly tumours (82%). Nevertheless, in the other 18% of lesions MRI-guided in-bore biopsy was negative. This negative result was confirmed in one patient via adenectomy. Although adenectomy does not exclude a tumour, the relevant central lesion in this patient should have been excised. Nevertheless, visually increased SI on the high *b*-value images is a sign of malignancy.

There was no significant difference regarding the ADC or the Gleason Score between lesions with or without increased SI on the high *b*-value images. Therefore increased SI is not an indication of a more aggressive tumour. In other studies the level of ADC reduction was demonstrated to be a criterion for a more aggressive tumour, as indicated by the higher Gleason Score [9, 10].

Generally the visualisation of the lesions on the high *b*-value images strongly depends on the *b* values used and cannot be generalised for other *b*-value selections. Nevertheless, the reason for the increased SI on the high *b*-value images of some lesions whether they were tumours or not remains elusive. When using the monoexponential model for the calculation of ADC, the ADC map is naturally influenced by the high *b*-value images [11]. As there was no difference in the ADC between lesions with or without increased SI, there must be another explanation. The greatest influence on SI on diffusion-weighted images is likely to be the T2 effect [12]. Because most lesions with increased SI were tumours with a hypointense appearance on the T2-weighted images, the impact of the T2 effect might be limited. DWI is also influenced by perfusion effects [13]. These effects mostly apply to low *b*-value images and not to the high *b*-value images ($b=1{,}000$ s/mm^2) used in the present study [14]. Another possible explanation might be that every tumour showed this increased SI depending on the level of *b* values used, owing to the further reduced signal of the surrounding tissue. Nevertheless, even benign lesions, in one patient even proven by adenectomy,

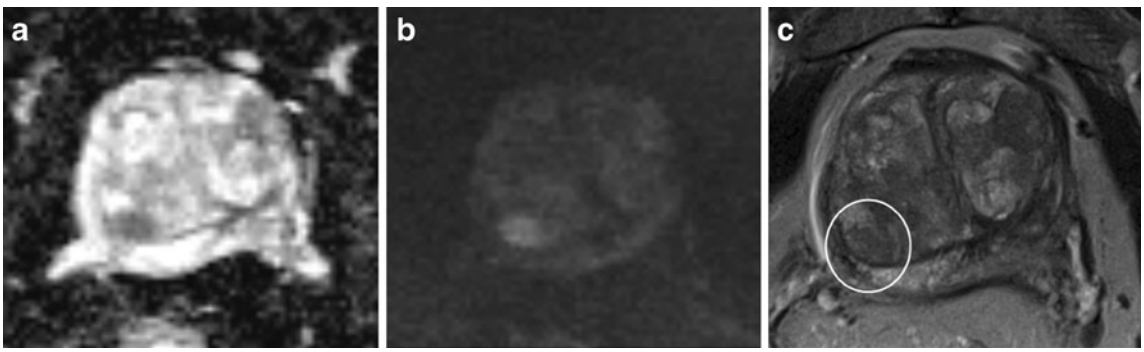

Fig. 2 A 70-year-old patient with a small central lesion with increased SI on the high *b*-value images and a negative biopsy. **a** ADC map with reduced SI; **b** increased SI on the high *b*-value image ($b=1{,}000$ s/mm^2); **c** corresponding T2-weighted image of the lesion

showed increased SI on the high *b*-value images. In this study, *b*-values up to a conventional clinical level were used [5]. The possible diagnostic advantage of using higher *b* values than 1,000 s/mm^2 in prostate MRI remains the subject of ongoing discussion [15, 16]. When using extremely high *b* values, the presence of different diffusion fractions can be measured influencing the SI on the high *b*-value images [17].

The present study is limited by its retrospective design, restricting the diagnostic accuracy of increased SI of prostate lesions at high *b* values. As the accuracy was not the main aim of the study, the retrospective design seemed appropriate. The selection of the lesions was based on T2-weighted imaging, DWI and DCE-MRI. Therefore, the prognostic significance of increased SI on the high *b*-value images could not be calculated separately. Further studies are needed to evaluate the diagnostic power of increased SI on high *b*-value images independently of the appearance of the lesion on the ADC map. Therefore, expressions like "true-positive findings, false-positive findings, true-negative findings and false-negative findings" were avoided in the present study.

A second limitation is that only one experienced radiologist evaluated the different lesions on the high *b*-value images whether a visually increased signal is present or not. Due to reduced signal-to-noise ratio on the high *b*-value images, this might be difficult in some cases. Nevertheless the measured SI on the high *b*-value images was significantly different between both groups. In conclusion, many prostatic lesions exhibit increased SI on high *b*-value diffusion-weighted prostate MRI. These lesions are mainly, but not exclusively, tumours. Nevertheless, increased signal intensity on high *b*-value images is a useful sign of malignancy.

References

1. Hoeks CM, Barentsz JO, Hambrock T et al (2011) Prostate cancer: multiparametric MR imaging for detection, localization, and staging. Radiology 261:46–66
2. Barentsz JO, Richenberg J, Clements R et al (2012) ESUR prostate MR guidelines 2012. Eur Radiol 22:746–757
3. Gibbs P, Tozer DJ, Liney GP, Turnbull LW (2001) Comparison of quantitative T2 mapping and diffusion-weighted imaging in the normal and pathologic prostate. Magn Reson Med 46:1054–1058
4. Arsov C, Blondin D, Rabenalt R et al (2012) Standardised scoring of a multi-parametric 3-T MRI for a targeted MRI-guided prostate biopsy. Urologe A 51:848–856
5. Dickinson L, Ahmed HU, Allen C et al (2011) Magnetic resonance imaging for the detection, localisation, and characterisation of prostate cancer: recommendations from a European consensus meeting. Eur Urol 59:477–494
6. Wittsack HJ, Lanzman RS, Mathys C et al (2010) Statistical evaluation of diffusion-weighted imaging of the human kidney. Magn Reson Med 64:616–622
7. Somford DM, Fütterer JJ, Hambrock T, Barentsz JO (2008) Diffusion and perfusion MR imaging of the prostate. Magn Reson Imaging Clin N Am 16:685–695, ix
8. Zelhof B, Pickles M, Liney G et al (2009) Correlation of diffusion-weighted magnetic resonance data with cellularity in prostate cancer. BJU Int 103:883–888
9. Hambrock T, Somford DM, Huisman HJ et al (2011) Relationship between apparent diffusion coefficients at 3.0-T MR imaging and Gleason grade in peripheral zone prostate cancer. Radiology 259: 453–461
10. Tamada T, Sone T, Jo Y et al (2008) Apparent diffusion coefficient values in peripheral and transition zones of the prostate: comparison between normal and malignant prostatic tissues and correlation with histologic grade. J Magn Reson Imaging 28:720–726
11. Quentin M, Blondin D, Klasen J et al (2012) Comparison of different mathematical models of diffusion-weighted prostate MR imaging. Magn Reson Imaging 30:1468–1474
12. Burdette JH, Elster AD, Ricci PE (1999) Acute cerebral infarction: quantification of spin-density and T2 shine-through phenomena on diffusion-weighted MR images. Radiology 212:333–339
13. Jacobs MA, Ouwerkerk R, Petrowski K, Macura KJ (2008) Diffusion-weighted imaging with apparent diffusion coefficient mapping and spectroscopy in prostate cancer. Top Magn Reson Imaging 19:261–272
14. Chandarana H, Lee VS, Hecht E, Taouli B, Sigmund EE (2011) Comparison of biexponential and monoexponential model of diffusion weighted imaging in evaluation of renal lesions: preliminary experience. Invest Radiol 46:285–291
15. Kitajima K, Kaji Y, Kuroda K, Sugimura K (2008) High b-value diffusion-weighted imaging in normal and malignant peripheral zone tissue of the prostate: effect of signal-to-noise ratio. Magn Reson Med Sci 7:93–99
16. Ueno Y, Kitajima K, Sugimura K et al (2013) Ultra-high b-value diffusion-weighted MRI for the detection of prostate cancer with 3-T MRI. J Magn Reson Imaging. doi:10.1002/jmri.23953
17. Le Bihan D (2008) Intravoxel incoherent motion perfusion MR imaging: a wake-up call. Radiology 249:748–752